Atmos. Chem. Phys., 11, 8965–8975, 2011
www.atmos-chem-phys.net/11/8965/2011/
doi:10.5194/acp-11-8965-2011

Atmospheric Chemistry and Physics

Isotope effects in N_2O photolysis from first principles

J. A. Schmidt[1], **M. S. Johnson**[1], **and R. Schinke**[2]

[1]Department of Chemistry, University of Copenhagen, Universitetsparken 5, 2100 Copenhagen Ø, Denmark
[2]Max-Planck-Institut für Dynamik und Selbstorganisation, 37073 Göttingen, Germany

Received: 20 May 2011 – Published in Atmos. Chem. Phys. Discuss.: 26 May 2011
Revised: 23 August 2011 – Accepted: 24 August 2011 – Published: 2 September 2011

Abstract. For the first time, accurate first principles potential energy surfaces allow N_2O cross sections and isotopic fractionation spectra to be derived that are in agreement with all available experimental data, extending our knowledge to a much broader range of conditions. Absorption spectra of rare N- and O-isotopologues ($^{15}N^{14}N^{16}O$, $^{14}N^{15}N^{16}O$, $^{15}N_2{}^{16}O$, $^{14}N_2^{17}O$ and $^{14}N_2^{18}O$) calculated using wavepacket propagation are compared to the most abundant isotopologue ($^{14}N_2^{16}O$). The fractionation constants as a function of wavelength and temperature are in excellent agreement with experimental data. The study shows that excitations from the 3rd excited bending state, $(0,3,0)$, and the first combination state, $(1,1,0)$, are important for explaining the isotope effect at wavelengths longer than 210 nm. Only a small amount of the mass independent oxygen isotope anomaly observed in atmospheric N_2O samples can be explained as arising from photolysis.

1 Introduction

Nitrous oxide, N_2O, is an important atmospheric trace gas. It is a potent greenhouse gas with a global warming potential 300 times greater than CO_2, and is currently the dominant anthropogenic emission depleting ozone (Ravishankara et al., 2009). The mixing ratio of N_2O has increased from 270 ppb (i.e. nmol/mol) in the preindustrial atmosphere to around 320 ppb today (Forster et al., 2007). Photolysis in the stratospheric UV window from ∼195 nm to 215 nm is responsible for about 90 % of the total N_2O loss. The remaining 10 % are removed through reactions with $O(^1D)$ (Prather et al., 2001, pp. 239), which is a major source of stratospheric NO which, in turn, catalytically removes ozone.

Correspondence to: J. A. Schmidt
(johanalbrechtschmidt@gmail.com)

The N_2O UV absorption cross section is centered at 183 nm and is Gaussian-like with superimposed structure at shorter wavelengths. Absorption in this band is caused by a transition from the electronic ground state to the first excited $^1A'$ state (Hopper, 1984):

$$N_2O(X^1A') + h\nu \rightarrow N_2O(2^1A') \rightarrow N_2(X^1\Sigma_g^+) + O(^1D). \quad \text{(R1)}$$

The first excited state ($^1A'$) is also referred to as the A-state. The broad Gaussian-like shape is typical for direct dissociation (Schinke, 1993), and the superimposed structure reflects large amplitude bending and NN stretching motion (Schinke et al., 2010; Schinke, 2011a). The dissociation dynamics lead to highly rotationally excited N_2 (Kawamata et al., 2006). The produced N_2 is vibrationally cold at the onset of the absorption cross section but becomes increasingly hotter with photon energy (Schmidt et al., 2011). The electronic transition is dipole forbidden in the linear geometry and the absorption cross section is relatively small for the vibrational ground state but grows with bending mode excitation. This makes the cross section quite sensitive to temperature (Selwyn and Johnston, 1981; Kawamata et al., 2006; Rontu Carlon et al., 2010; Schinke, 2011a,b).

Photolysis has a strong influence on the isotopic composition of N_2O in the atmosphere (Kim and Craig, 1993; Toyoda et al., 2001). Stratospheric N_2O, compared to its tropospheric counterpart, is enriched in heavy isotopes (Moore, 1974; Rahn and Wahlen, 1997). The tropospheric sources have been found to be depleted in both ^{15}N and ^{18}O (Kim and Craig, 1993). Early laboratory measurements at 185 nm found no strong fractionation and called the importance of photolysis into question (Johnston et al., 1995). However, Yung and Miller (1997) showed, using a qualitative model, that photolysis in the stratosphere will significantly enrich the remaining N_2O. The model took into account that heavy isotopologues, i.e. $^{14}N_2{}^{18}O$, have a smaller ground state vibrational energy and the overall absorptions band of these isotopologues therefore tend to be shifted to higher energies.

Published by Copernicus Publications on behalf of the European Geosciences Union.

The absorption cross section (and the rate of photolysis) is therefore smaller for the heavy isotopologues on the low-energy side of the cross section. Since N_2O is primarily photolysed on the low energy side (at $\lambda > 195$ nm) this causes the remaining pool of N_2O to be enriched in heavy isotopes. Laboratory experiments (cf. Kaiser et al., 2003; von Hessberg et al., 2004) later found photolysis to be even more enriching than first predicted by the Yung and Miller model.

At the same time the first evidence of a small O-isotope anomaly appeared with the measurement of a $\Delta^{17}O$ of about 1‰ in atmospheric N_2O samples (Cliff and Thiemens, 1997). The origin of this anomaly is not well understood (McLinden et al., 2003; Liang and Yung, 2007; Kaiser and Röckmann, 2005). Experiments performed using Sb-lamps at room temperature found $\Delta^{17}O = 0$ ‰ within experimental error and photolysis is therefore not believed to contribute to the anomaly (Röckmann et al., 2001b). A number of non-standard atmospheric N_2O sources have been suggested (Röckmann et al., 2001b; McLinden et al., 2003; Kaiser et al., 2004; Kaiser and Röckmann, 2005; Liang and Yung, 2007), e.g. $O(^1D)$+N_2, NH_2+NO_2 and N+NO_2, which could transfer the anomaly from ozone (which contains a large O-isotope anomaly). The magnitudes of these sources are not well known. Röckmann et al. (2001b) estimated that the NH_2+NO_2 reaction could, by itself, explain the anomaly if about 3 % of the global N_2O originated from this reaction. This estimate was later refined by the construction of an isotope budget (Kaiser and Röckmann, 2005) and an atmospheric model (Liang and Yung, 2007) that included the different non-standard sources. In the isotope budget by Kaiser and Röckmann (2005) the NH_2+NO_2 contribution to the global production is only about 0.5 %. Yoshida and Toyoda (2000) used the site specific ^{15}N enrichment (i.e. $^{15}N^{14}N^{16}O$ vs. $^{14}N^{15}N^{16}O$) observed in field measurements to constrain the atmospheric N_2O budget.

There have been several theoretical studies on isotopic fractionation in N_2O photolysis (Johnson et al., 2001; Nanbu and Johnson, 2004; Liang et al., 2004; Prakash et al., 2005; Chen et al., 2008, 2010). The ab initio study by Daud et al. (2005) did not consider isotope effects. The isotope study by Nanbu and Johnson (2004) was the only one to be based entirely on first principles. This work together with earlier studies of Johnson et al. (2001) and Yung and Miller (1997) were helpful in understanding the main aspects of the fractionation. However, the comparison with experimental results was less convincing.

Better agreement with experiments was obtained by Marcus and co-workers (Prakash et al., 2005; Chen et al., 2008, 2010). These studies were based on an approximation known as the *reflection principle* (Schinke, 1993, ch. 6) and the diffuse structure and (less important) high energy side of the cross section was not reproduced. These studies clearly illustrated the importance of having a reliable description of the vibrational states of the electronic ground state. The latest study by this group used an accurate semi-empirical ground state Potential Energy Surface (PES) to obtain anharmonic vibrational wavefunctions which could be considered nearly exact together with an ab initio excited state PES and a Transition Dipole Moment surface (TDM). Note that the semi emperical PES was based on spectroscopic experimental data that are independent of the present isotopic fractionation data. The calculated fractionation constants were mostly in quantitative agreement with experimental results. To obtain this good agreement it was necessary to shift the cross sections about 800 cm^{-1}; the origin of this small shift was most likely inaccuracies in the excited state PES.

This is the first theoretical study, based entirely on first principles, to accurately describe all aspects of isotopic fractionation in N_2O photolysis. No artificial broadening or shifting of the results is performed and they can therefore be considered as pure ab initio results. The results are in good agreement with the latest reflection principle based model (Chen et al., 2010) and accurately describe the isotopic fractionation observed in broadband photolysis experiments (Röckmann et al., 2001a; Kaiser et al., 2003) and also the detailed temperature dependence observed in other experiments (Kaiser et al., 2002). We show that even highly excited vibrational states (e.g. the 3rd excited bending state and the first combination state) are important for understanding fractionation at longer wavelengths. We also find that photolysis is mass-dependent for $\lambda > 195$ nm and can for the first time account for the observation that the three-isotope exponent β changes with wavelength.

2 Calculations

2.1 Potential energy surfaces

The PESs for the ground state and the excited state, V_X and V_A, were calculated using the multi-configuration reference internally contracted configuration interaction (MRCI) theory (Werner and Knowles, 1988; Knowles and Werner, 1988) based on wave functions obtained by state-averaged full-valence complete active space self consistent field (CASSCF) calculations (Werner and Knowles, 1985; Knowles and Werner, 1985). The augmented correlation consistent polarized valence quadruple zeta (aug-cc-pVQZ) basis set of Dunning Jr. (1989) was employed. The Davidson correction was applied in order to approximately account for contributions of higher excitations and for size-extensive energies (Langhoff and Davidson, 1974). The corresponding TDM (μ_{XA}) was calculated at the same level of theory. Further details are given by Schinke (2011a). The PESs and the TDM were calculated as functions of the Jacobi coordinates R (distance from O to the center of mass of NN), r (NN bond length), and γ (angle between R and r). For isotopomers including different nitrogen isotopes a coordinate transformation between the different sets of Jacobi coordinates is mandatory.

The PESs and TDM are currently the most accurate ab initio surfaces available for N_2O. They have an excellent track record; they were used to obtain the N_2O UV absorption cross section (Schinke et al., 2010; Schinke, 2011a) which, including the vibrational structure, was in good agreement with experiments. They were also used to investigate the temperature dependence (Schinke, 2011b) of the absorption cross section and the energy partitioning in the products (Schmidt et al., 2011) and again the agreement with experimental data was excellent. The overall scaling factor of ∼1.4 necessary to match the absolute value of the experimental cross section in (Schinke et al., 2010; Schinke, 2011a) is of no relevance in the present study, because only ratios of cross sections are considered.

2.2 Quantum mechanical calculations

The absorption cross sections were calculated using the time-dependent approach (Schinke, 1993, ch. 4). The triatomic system was described using the Jacobi coordinates defined in Sect. 2.1. Wave packets were propagated on the A-state PES and the resulting autocorrelation functions were used to calculate the cross sections. An initial wave packet at $t = 0$, $\Phi(R, r, \gamma; 0)$, was defined as the product of a vibrational wave function of the X-state, $\Psi_{(v_1,v_2,v_3)}$, and the modulus of the TDM, μ_{XA}. The propagation was performed by expanding the propagator in Chebychev polynomials (Tal-Ezer and Kosloff, 1984). Propagation was terminated after 250 fs. The pseudospectral scheme presented by Le Quéré and Leforestier (1990) was employed. In this scheme the action of the radial part, i.e. R and r, of the kinetic energy operator on the wave packet is evaluated via the Fourier method (Kosloff and Kosloff, 1983), while the angular part is evaluated by transforming between a grid representation and an associated Legendre polynomial, $P_l^m(\cos(\gamma))$, basis set representation. The following grid parameters were employed: 400 and 140 equally spaced points in the intervals $2\,a_0 \le R \le 13.97\,a_0$ and $1.6\,a_0 \le r \le 5.77\,a_0$ respectively (where a_0 is the Bohr radius), and 256 angle grid points between $\gamma = 0$ and $\gamma = 180°$. To prevent the wave packet from reflection at the edge of the grid, absorbing boundaries were employed for $R > 10\,a_0$ and $r > 4.2\,a_0$.

Calculations were performed for the vibrational ground state, $(0,0,0)$, the first four excited bending states, $(0,1^1,0)$, $(0,2,0)$, $(0,3^1,0)$, $(0,4,0)$, the first excited stretching states, $(1,0,0)$, $(0,0,1)$, and the first combination state, $(1,1^1,0)$. The vibrational wave functions of the X-state were obtained by propagating a trial wave packet in imaginary time (Kosloff and Tal-Ezer, 1986). When obtaining the excited states (except $(0,1^1,0)$) it was necessary to continuously project out components of lower energy from the trial wave packet. All calculations involving $(0,0,0)$, $(0,2,0)$, $(0,4,0)$, $(1,0,0)$ and $(0,0,1)$ were done using Legendre polynomials (i.e. $m = 0$) while calculations involving $(0,1^1,0)$, $(0,3^1,0)$ and $(1,1^1,0)$ were done using associated Legendre polynomials with $m =$

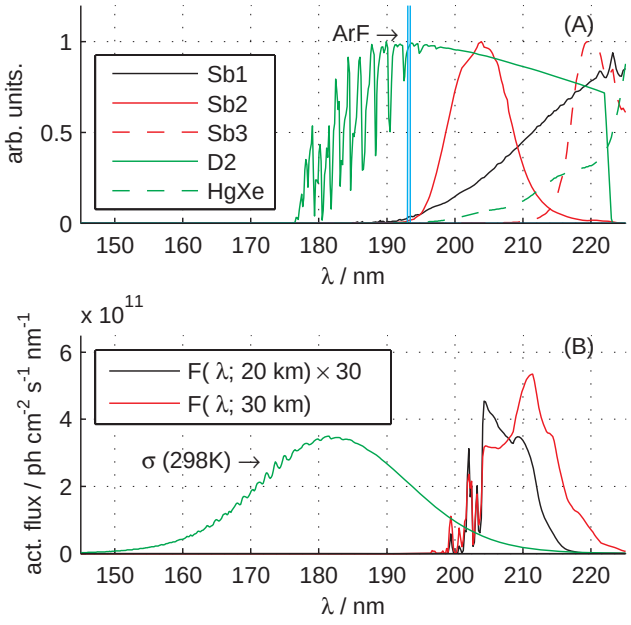

Fig. 1. Panel **(A)**: The spectra of the various lamps used in the broadband photolysis studies of Kaiser et al. (2002, 2003) and Röckmann et al. (2001a,b). "Sb1", "Sb2" and "Sb3" refer to Sb lamp without filter, with 200 nm filter and 220 nm filter, respectively. The position of the ArF excimer laser line used in the latter study is also shown. Panel **(B)**: The N_2O cross section compared to the actinic flux $F(\lambda)$ at different altitudes.

1. A modified version of the `WavePacket 4.6` program package (Schmidt and Lorenz, 2009) was used to perform the quantum calculations.

2.3 Photochemical calculations

When comparing the results of this study with experimental studies performed using broadband light sources, e.g. Sb-lamp or the sun, it was necessary to calculate the rate of photolysis,

$$j = \int \mathrm{d}\lambda\, \sigma(\lambda) F(\lambda) \phi(\lambda), \qquad (1)$$

where $F(\lambda)$ is the quantity of light available for photolysis at given wavelength, e.g. the actinic flux in the case of atmospheric photolysis. The yield of dissociation, $\phi(\lambda)$, is set to unity in accordance with experimental results (Simonaitis et al., 1972) and since the photodissociation process is direct (Schinke et al., 2010; Schinke, 2011a) and essentially all of the wave packet has dissociated after 250 fs.

2.3.1 Lamp spectral data

The spectral data for the various light sources used in the experimental studies (Kaiser et al., 2002, 2003; Röckmann et al., 2001a,b) was obtained from J. Kaiser and a selection

Table 1. Vibrational energies given in cm^{-1} of $^{14}N_2{}^{16}O$, with $E'_i = E_i - E_{(0,0,0)}$. The experimental excitation energies are the gas phase values cited in Łapiński et al. (2001) and HZPE $= 0.5E'_{(1,0,0)} + E'_{(0,1,0)} + 0.5E'_{(0,0,1)}$ is a harmonic estimate of the zero point energy.

	HZPE	$E_{(0,0,0)}$	$E'_{(0,1,0)}$	$E'_{(0,2,0)}$	$E'_{(0,3,0)}$	$E'_{(0,4,0)}$	$E'_{(1,0,0)}$	$E'_{(1,1,0)}$	$E'_{(0,0,1)}$
This study	2323.0	2388.0	569.8	1148.2	1727.9	2293.8	1291.5	1858.2	2214.9
Experiment	2343.2		588.8	1168.1			1284.9	1880.3	2223.8

is shown in Panel a of Fig. 1. The D_2 lamp data is a convolution of the spectral radiant intensity of a D_2 lamp with the transmission function of a Hamamatsu silica window and the O_2 Schumann-Runge band (see Kaiser et al. (2003)). The Sb-lamp was used both with and without band pass interference filters (Melles Griot) centered at 4 different wavelengths; 200 nm, 207 nm, 214 nm and 220 nm. The filter functions used in this study were measured by Kaiser et al. (2003).

2.3.2 Actinic flux data

Actinic flux data at 0.1 nm resolution at various altitudes were obtained from McLinden et al. (2002) and are shown together with the N_2O absorption cross section in Panel b of Fig. 1.

2.4 Isotopic fractionation

The enrichment of a given isotope, e.g. ^{18}O, is commonly (Assonov and Brenninkmeijer, 2005) quantified in terms the relative isotope ratio difference (or isotope delta) defined as,

$$\delta^{18}O = \frac{^{18}R}{^{18}R_{\mathrm{ref}}} - 1, \tag{2}$$

where $^{18}R_{\mathrm{ref}}$ is the ^{18}O:^{16}O ratio in a reference, with Vienna Standard Mean Ocean Water (VSMOW) being a typical reference for oxygen. The $^{14}N_2{}^{18}O$ isotopic fractionation as function of wavelength is commonly quantified using the *fractionation constant* (cf. von Hessberg et al., 2004; Johnson et al., 2001; Nanbu and Johnson, 2004; Prakash et al., 2005; Chen et al., 2008, 2010),

$$^{18}\epsilon(\lambda) = \frac{^{18}\sigma(\lambda)}{\sigma(\lambda)} - 1, \tag{3}$$

where $\sigma(\lambda)$ and $^{18}\sigma(\lambda)$ are the $^{14}N_2{}^{16}O$ and $^{14}N_2{}^{18}O$ cross sections respectively, and analogous definitions apply for the other isotopes. The fractionation constant can also be defined for broadband photolysis (cf. Kaiser et al., 2004),

$$^{18}\epsilon = \frac{^{18}j}{j} - 1. \tag{4}$$

For a first order process, like photolysis, the concentration of the reactant decays exponentially in time. The ratio of a rare isotopologue, i.e. $^{14}N_2{}^{18}O$, to the most abundant can therefore be expressed as,

$$\frac{[^{14}N_2{}^{18}O]_t}{[^{14}N_2{}^{16}O]_t} = \frac{[^{14}N_2{}^{18}O]_0}{[^{14}N_2{}^{16}O]_0}\, e^{(j-^{18}j)t}, \tag{5}$$

where $[X]_t$ are the concentrations at a time t. By defining the variable f as the remaining fraction of unphotolysed $^{14}N_2{}^{16}O$, i.e.,

$$f = \frac{[^{14}N_2{}^{16}O]_t}{[^{14}N_2{}^{16}O]_0} = e^{-jt}, \tag{6}$$

a simple expression for the isotope delta ($\delta^{18}O$) as a function of f can be obtained,

$$\delta^{18}O = \left(\frac{^{18}R_0}{^{18}R_{\mathrm{ref}}}\right) f^{^{18}\epsilon} - 1, \tag{7}$$

where $^{18}R_0$ is the initial isotope ratio.

Early experimental studies (Cliff and Thiemens, 1997; Röckmann et al., 2001b) quantified the oxygen isotope anomaly using,

$$\Delta^{17}O = \delta^{17}O - 0.515\,\delta^{18}O, \tag{8}$$

while the later study of Kaiser et al. (2004) suggested using $\Delta^{17}O^*$ defined as,

$$\Delta^{17}O^* = \frac{1+\delta^{17}O}{(1+\delta^{18}O)^{0.516}} - 1, \tag{9}$$

and also suggested using the *three-isotope exponent*,

$$\beta = \frac{\ln(^{17}\epsilon + 1)}{\ln(^{18}\epsilon + 1)}, \tag{10}$$

to determine if photolysis (or any other process) is anomalous. If β is either smaller than 0.50 or greater than 0.53 then the process is considered to be anomalous (Kaiser et al., 2004; Assonov and Brenninkmeijer, 2005). The isotope delta, fractionation constant, and $\Delta^{17}O$ are usually denoted in per mil (‰).

3 Results and comparison with experiments

Table 1 compares the vibrational energies obtained in this study to experimental results. The calculated vibrational excitation energies, E'_i, are in most cases smaller than the

Table 2. Isotopic shift in vibrational energies in cm^{-1}. Experimental gas phase values cited in Łapiński et al. (2001) are given in parenthesis. The shifts are defined as $\Delta^{18}E = E(^{14}N_2{}^{16}O) - E(^{14}N_2{}^{18}O)$ and $\Delta^{18}E_i' = E_i'(^{14}N_2{}^{16}O) - E_i'(^{14}N_2{}^{18}O)$ for ^{18}O and analogously for other isotopes.

	ΔHZPE	$\Delta E_{0,0,0}$	$\Delta E'_{0,1,0}$	$\Delta E'_{0,2,0}$	$\Delta E'_{0,3,0}$	$\Delta E'_{1,0,0}$	$\Delta E'_{1,1,0}$	$\Delta E'_{0,0,1}$
$^{14}N^{15}N^{16}O$	38.6 (38.7)	38.0	13.5 (13.4)	23.3 (23.8)	34.4	5.3 (4.5)	20.6	44.8 (46.1)
$^{15}N^{14}N^{16}O$	21.4 (22.0)	23.0	3.5 (3.5)	8.6 (8.1)	12.7	14.4 (15.0)	17.2	21.4 (22.2)
$^{15}N_2{}^{16}O$	60.7 (61.2)	61.3	17.0 (16.9)	31.5 (31.6)	46.6	19.6 (19.6)	38.2 (37.9)	67.8 (69.1)
$^{14}N_2{}^{17}O$	13.9 (14.4)	15.3	2.4 (2.4)	7.0 (6.6)	10.6	19.8 (20.2)	20.8	3.2 (3.7)
$^{14}N_2{}^{18}O$	26.6 (27.1)	29.0	4.6 (4.6)	13.8 (13.0)	20.9	37.4 (38.0)	39.1	6.6 (7.1)

experimental values with the biggest deviation being about 20 cm^{-1}. The calculated isotopic energy shifts are compared to experimental data in Table 2. The deviation from experiments is small, usually on the order a of few tenths of a cm^{-1}. The largest deviations are seen for $(0,0,1)$.

The cross sections for the vibrational states are shown in Panel a of Fig. 2. The overall magnitude increases with bending excitation as discussed elsewhere (Schinke, 2011a; Rontu Carlon et al., 2010; Johnson et al., 2001). The bimodal structure for $(1,0,0)$ and $(1,1,0)$ reflects the node of the respective wavefunctions along the dissociation coordinate R (Schinke, 1993). Panel b shows the cross sections multiplied by the Boltzmann weighting factor at $T = 300$ K. The weighting factor for $(0,0,1)$ is so small that $w_{(0,0,1)}\sigma_{(0,0,1)}$ lies outside the range plotted in Panel b. In the important region around 210 nm the contributions to the total cross section at 300 K are $1:1:0.5:0.1:0.05:0.025:0.01$ for $(0,0,0)$, $(0,1,0)$, $(0,2,0)$, $(0,3,0)$, $(1,0,0)$, $(1,1,0)$ and $(0,4,0)$ respectively. The contribution from the 3rd bending excitation is significant at room temperature; we note that ignoring this state changes the calculated broadband photolysis fractionation constants by up to 20 ‰. For the isotopic calculations the $(0,4,0)$ and $(0,0,1)$ vibrational states can be ignored because the weighted cross sections are so small. Daud et al. (2005) considered several electronically excited states and found that the absorption cross section for the $X^1A' \rightarrow 1^1A''$ transition consists of two broad overlapping Gaussians peaking around 170 and 190 nm. The magnitude of the $X^1A' \rightarrow 1^1A''$ cross section was typically 1 % or less of the magnitude of the $X^1A' \rightarrow 2^1A'$ cross section. This suggests that the $1^1A''$ electronic state and the 4th excited bending state are about equally (un)important for describing the total cross section at 300 K and the $1^1A''$ electronic state is therefore not included in this study. At 233 K the contributions around 210 nm go as $1:0.5:0.1:0.01:0.01:0.002:0.0005$, and a fair representation could have been obtained by only considering the ground state and the first two excited bending states.

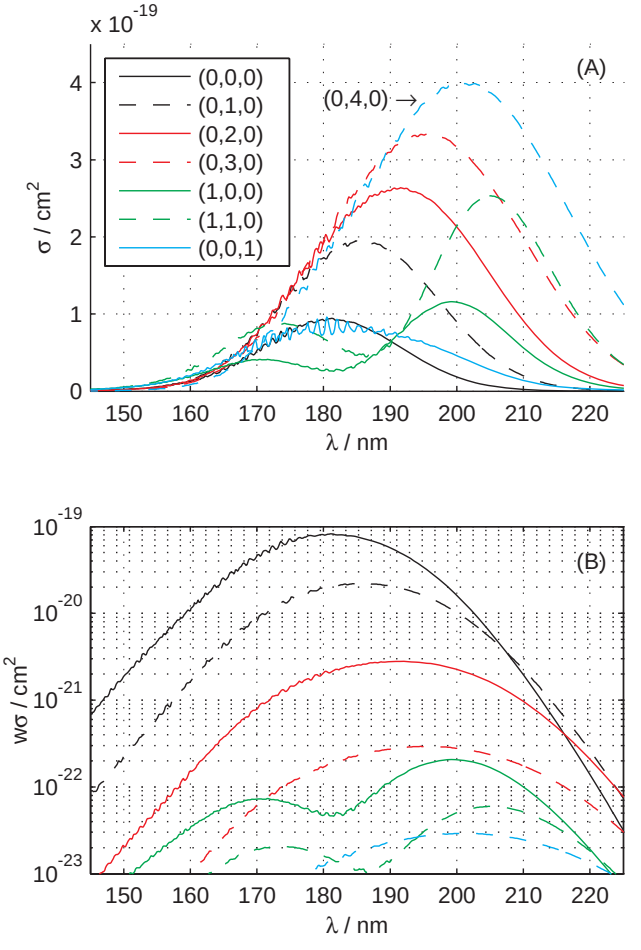

Fig. 2. Panel **(A)**: The N_2O cross section for various initial vibrational states. Panel **(B)**: Cross sections for the various initial states multiplied by the Boltzmann weighting factor $w_i = Q^{-1}(1+v_2)\exp(-E_i/(k_BT))$ with $T = 300$ K and Q being the partition function.

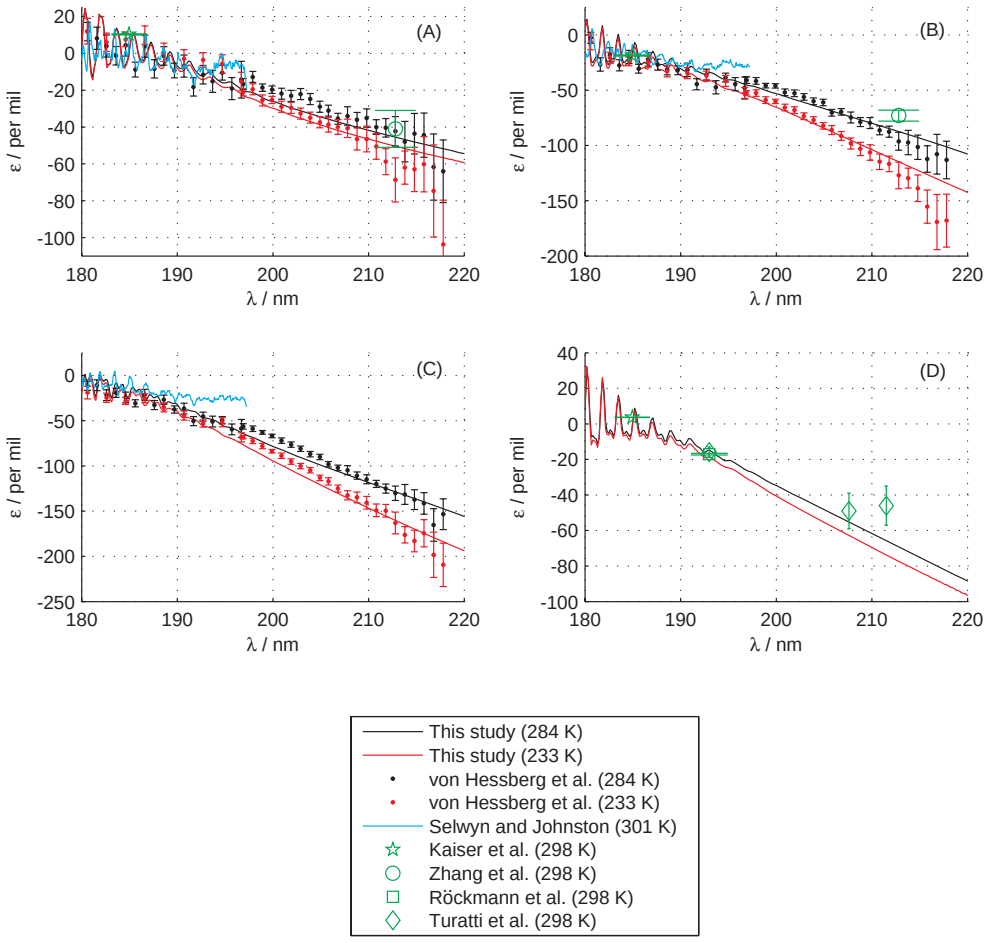

Fig. 3. The fractionation constants for $^{15}N^{14}N^{16}O$ (Panel **A**), $^{14}N^{15}N^{16}O$ (Panel **B**), $^{15}N_2{}^{16}O$ (Panel C) and $^{14}N_2{}^{18}O$ (Panel D) at different temperatures compared to experimental results of von Hessberg et al. (2004), Selwyn and Johnston (1981), Kaiser et al. (2003), Zhang et al. (2000), Röckmann et al. (2000) and Turatti et al. (2000). The legend applies to all panels, however the results of this study in Panel d were calculated at 300 K (black) and 220 K (red).

3.1 Monochromatic photolysis

Figure 3 shows the fractionation constant as a function of wavelength compared to the spectroscopic measurements of Selwyn and Johnston (1981) and von Hessberg et al. (2004). The results of four single-wavelength photolysis experiments (Kaiser et al., 2003; Zhang et al., 2000; Röckmann et al., 2000; Turatti et al., 2000) are also shown. Overall, the agreement with experimental results is excellent. Compared to the spectroscopic results of von Hessberg et al. (2004), our results slightly underestimate the magnitude of the fractionation at wavelengths longer than 212 nm. However, our results overestimate the magnitude of fractionation compared to single-wavelength photolysis based experimental results (Zhang et al., 2000; Turatti et al., 2000). The results of Selwyn and Johnston (1981) are generally believed to be inaccurate at longer wavelengths: the authors wrote: "at low energies the isotope shift and the random experimental error are about equal".

The N- and O-isotopic fractionation becomes increasingly negative with increasing wavelength. This behavior has been explained by several groups (Yung and Miller, 1997; Johnson et al., 2001; Nanbu and Johnson, 2004; Liang et al., 2004; Prakash et al., 2005) and arises because: (a) The heavy isotopes of N_2O have a smaller ZPE which shifts their cross sections to higher energies, making photolysis slower on the low energy side. (b) The wavefunctions of the heavy isotopes are narrower making the cross sections narrower and in turn making the rate of photolysis decrease more rapidly on the low energy side. The "narrowing" of the heavy isotope wavefunctions (in particular along the bending degree of freedom) also decreases the integrated cross section and shifts the cross section to higher energies. The latter is a consequence of a growing excitation energy because V_A increases when going towards a linear geometry.

The Yung and Miller model (1997) included the first effect but ignored the second which led the model to underestimate the magnitude of the fractionation. Later theoretical studies

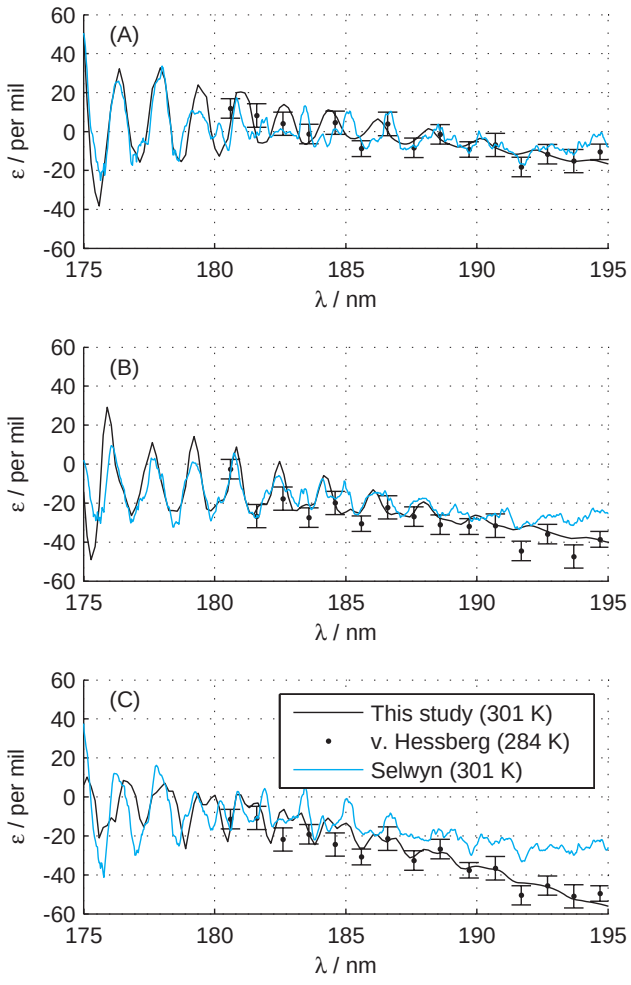

Fig. 4. The fractionation constants for $^{15}N^{14}N^{16}O$ (Panel **A**), $^{14}N^{15}N^{16}O$ (Panel **B**), $^{15}N_2{}^{16}O$ (Panel C) compared to experimental results of von Hessberg et al. (2004), and Selwyn and Johnston (1981). The legend in Panel C applies to all panels. A blue shift of 300 cm^{-1} (about 1 nm) has been applied to our results in all panels of this figure.

(Johnson et al., 2001; Nanbu and Johnson, 2004; Prakash et al., 2005; Chen et al., 2008, 2010) included both effects. The temperature effects of the N- and O-isotope fractionation will be discussed below.

Figure 4 gives a more detailed view of the fractionation constants in the structured region at $\lambda < 195$ nm. The structure predicted by this study is slightly out of phase with the structure measured by Selwyn and Johnston (1981). The results of this study can be brought in phase with experimental results by either applying a blue shift of ~ 1 nm or a red shift of ~ 0.5 nm to our results. As seen in Fig. 4 the spacing between the peaks and the overall pattern is well reproduced. Results at low temperatures are not shown since both this study and the study by Selwyn and Johnston (1981) finds the fractionation constants at 301 K and 213 K to coincide almost perfectly in the structured region. This is not surprising since photolysis in this region is dominated by transitions from the vibrational ground state (see Fig. 2) and the population of this state is not very sensitive to temperature.

The calculated three-isotope exponent is shown in Fig. 5 and compared to available experimental data. For stratospheric photolysis at wavelengths longer than 195 nm the calculated β is around 0.526 and is therefore always *mass-dependent* (in the sense that $0.50 \leq \beta \leq 0.53$). Our three-isotope exponent is slightly larger than the value of 0.518 derived by Kaiser et al. (2004) for Sb-lamp photolysis, and smaller than the *anomalous* value of 0.537 obtained in the most recent reflection principle based study of Chen et al. (2010). At wavelengths shorter than 200 nm the cross sections display diffuse vibrational structure due to large amplitude bending and NN stretching motion (Schinke et al., 2010; Schinke, 2011a), causing large oscillations in the fractionation constants and the three-isotope exponent. The measured ArF laser photolysis (193.3 nm) three-isotope exponent coincides almost perfectly with a calculated dip in β. The calculated value of beta is only very slightly dependent on temperature, changing by a few thousandths as temperature is decreased from 300 to 220 K.

The three-dimensional chemical transport model of McLinden et al. (2003) shows that a mass-dependent source of N_2O in equilibrium with an isotopically fractionating stratospheric sink will give a $\Delta^{17}O$ value of 0.3 ‰ for $\beta = 0.545$ and 0.0 ‰ for $\beta = 0.515$. An interpolation for our result of $\beta = 0.526$ predicts that stratospheric photolysis will result in an oxygen isotope anomaly of 0.1 ‰ and therefore cannot by itself explain the tropospheric anomaly of ca. 1 ‰.

3.2 Broadband photolysis

Table 3 compares the calculated broadband fractionation constants with experimental data (Röckmann et al., 2001a; Kaiser et al., 2003). In general the agreement is good. Most of the broadband photolysis experiments were centered at long wavelengths where many excited vibrational states contribute to the cross section at room temperature (see Fig. 2). The contribution from relatively highly excited states like $(0,3,0)$ and $(1,0,0)$ are therefore important for describing the broadband photolysis fractionation. For instance, ignoring the 3rd excited bending (1st excited stretch) state increases the deviation between experiment and theory by up to 21 ‰ (10 ‰). The bending excitation has a larger effect on $^{14}N^{15}N^{16}O$, i.e. the centrally substituted case, while the stretching excitation is most important for describing $^{14}N_2{}^{18}O$. The contributions from $(1,0,0)$ and $(1,1,0)$ to the total cross section at 300 K are comparable at 214 nm and 220 nm; as is the "isotope-effect" exemplified by the energy shift, $\Delta E_i'$, which is 39.1 cm^{-1} and 37.4 cm^{-1} in the case of $^{14}N_2{}^{18}O$ for $(1,1,0)$ and $(1,0,0)$ respectively. The inclusion of the first combination band changed the predicted fractionation factors by as much as 8 ‰.

Table 3. Fractionation constants for photolysis with broadband light sources. Results obtained without including $(0,3,0)$ and $(1,1,0)$ are given in brackets and experimental results of Röckmann et al. (2001a)[a] and Kaiser et al. (2003)[b] are given in parenthesis.

	$^{456}\epsilon$ / ‰			$^{546}\epsilon$ / ‰			$^{18}\epsilon$ / ‰		
Sb lamp	−57.6	[−62.2]	(−51.2 ± 1.6)[a]	−29.0	[−29.9]	(−21.4 ± 1.1)[a]	−43.0	[−44.1]	(−33.1 ± 1.1)[a]
Sb 200nm filter	−53.8	[−57.0]		−27.6	[−28.4]		−39.0	[−40.1]	(−43 ± 8)[b]
Sb 214nm filter	−84.2	[−97.7]	(−74 ± 13)[b]	−46.0	[−48.9]	(−41 ± 7)[b]	−72.5	[−76.5]	(−52 ± 9)[b]
Sb 220nm filter	−96.7	[−116.2]	(−95 ± 7)[b]	−51.9	[−55.9]	(−43 ± 3)[b]	−84.6	[−90.3]	(−61 ± 5)[b]
HgXe lamp	−70.9	[−78.2]	(−69.5 ± 2.8)[b]	−36.8	[−38.1]	(−28.1 ± 2.1)[b]	−56.5	[−57.8]	(−46.9 ± 1.9)[b]
D_2 lamp	−29.7	[−30.7]	(−31.4 ± 0.3)[b]	−7.4	[−7.6]	(−8.4 ± 0.4)[b]	−13.1	[−13.4]	(−15.9 ± 0.1)[b]

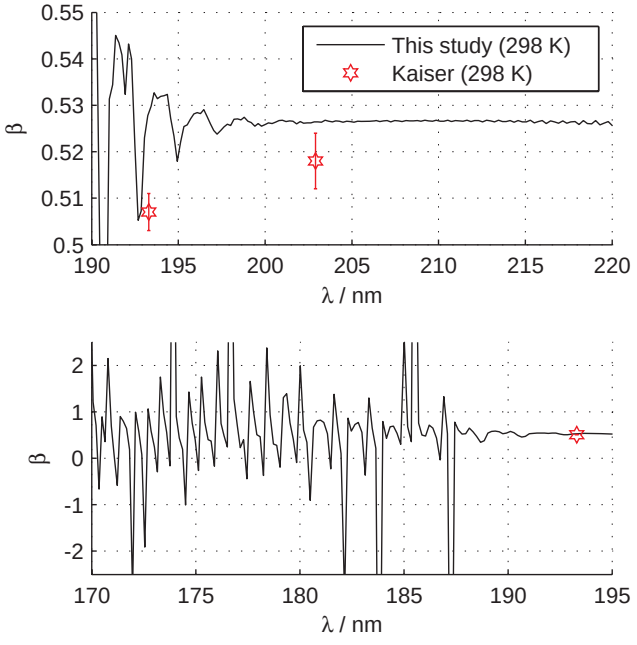

Fig. 5. The three-isotope exponent (see Eq. 10) at room temperature compared to ArF ($\lambda = 193.3$ nm) and Sb-lamp ($\lambda \sim 202$ nm) experimental results of Kaiser et al. (2004)

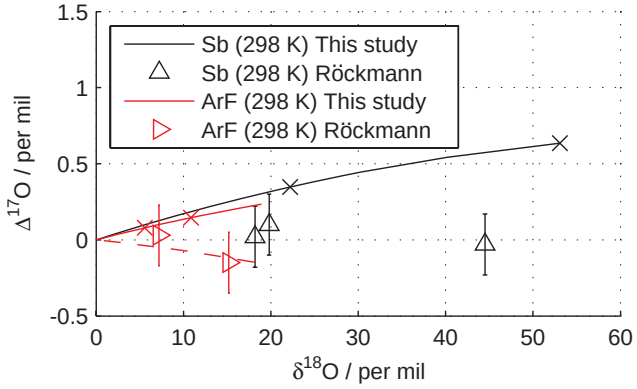

Fig. 6. The evolution of $\delta^{18}O$ and $\Delta^{17}O$ as the fraction of remaining reactant (f) decreases. The $\delta^{18}O$ and $\Delta^{17}O$ of this study are calculated using Eqs. (7) and (8). All lines run from $f = 1.0$ to 0.3 (i.e. from 0 % to 70 % conversion). The black × mark $f = 0.6$ and $f = 0.3$ while the red × mark $f = 0.7$ and $f = 0.5$. The experimental results of Röckmann et al. (2001b) are at about the same yield of reaction. The broken red line is monochromatic photolysis at 192.8 nm.

Figure 6 shows $\delta^{18}O$ vs. $\Delta^{17}O$ for different reaction yields. Equations (7) and (8) are used to obtain $\delta^{18}O$ and $\Delta^{17}O$. This definition of $\Delta^{17}O$ was also used in the experimental studies of Cliff and Thiemens (1997) and Röckmann et al. (2001b). The Sb-lamp results of this study, despite being mass-dependent in terms of $\beta = 0.526$, yield an oxygen isotope anomaly of up to about $\Delta^{17}O = 0.6$ ‰. However, laboratory Sb-lamp measurements of Röckmann et al. (2001b) found photolysis to yield $\Delta^{17}O = 0 \pm 0.2$ ‰. The 0.6 ‰ deviation between theory and experiments could be a result of small inaccuracies in the PESs or TDM. This study finds that photolysis at 193.3 nm (the ArF wavelength) yields a small positive anomaly of around $\Delta^{17}O = 0.2$ ‰ at $f = 0.3$. The experimental results show no anomaly within the error bars, but have a negative tendency due to $\beta = 0.507 < 0.515$ for this light source (Kaiser et al., 2004). Figure 6 also shows the development of $\delta^{18}O$ and $\Delta^{17}O$ for photolysis at 192.8 nm, the λ for which β has a local minima (see Fig. 5). The result of photolysis at 192.8 nm is strikingly similar to the experimental ArF results. An inaccuracy of about 0.5 nm (134 cm^{-1}) in the calculated PES is not unrealistic and the ArF laser line would perfectly match the "dip" in β. The difference in three-isotope exponent between the two light sources would then be due to a coincidental matching of the ArF laser frequency with the "dip" in β due to the structure caused by large amplitude bending and NN stretching motion.

3.3 Temperature dependence

The variation of the isotopic fractionation with temperature is shown in Fig. 3 and in greater detail in Fig. 7. As a common trend, the magnitude of the isotopic fractionation increases with decreasing temperature. This was first predicted qualitatively by the early theoretical study of Johnson et al. (2001) and later confirmed by experiments (Kaiser et al.,

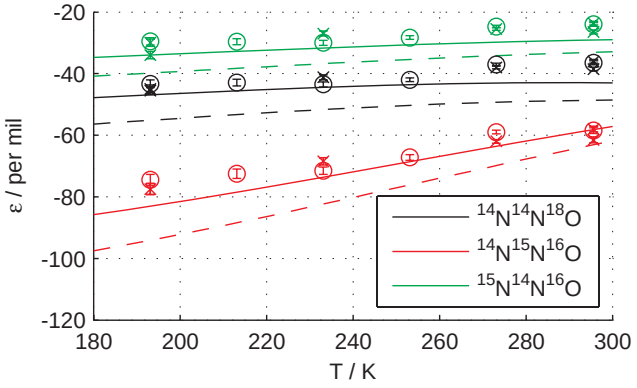

Fig. 7. The Sb-lamp fractionation constant vs. temperature. The fractionation constants of this study are calculated using Eqs. (1) and (4). Broken and solid lines are the results of this study with and without 207 nm filter respectively, while ∘ and × mark the experimental data of Kaiser et al. (2002) also with and without 207 nm filter respectively.

2002; von Hessberg et al., 2004). The calculated temperature dependence is in good agreement with experimental observations. As seen in Fig. 2 populating the excited vibrational states increases the cross section at the low energy side. The excited vibrational states of the heavy isotopes of N_2O are lower in energy compared to light N_2O and are therefore populated more quickly with increasing temperature, thus enhancing the low energy side of the cross section and counteracting the negative fractionation.

As seen in Fig. 7, our results predict that the 207 nm bandpass filter lowers the fractionation by about 5–15 ‰. However the experiments find that the filter has almost no effect on the fractionation. This deviation could be a result of inaccuracies in the calculated cross sections at longer wavelengths.

4 Conclusions

The photodissociation of N_2O in the first absorption band leads to strong N- and O-isotopic fractionation. The magnitude of the fractionation depends on photolysis energy (wavelength) and temperature

The isotopic fractionation in N_2O photolysis was studied using quantum mechanical wave packet calculations and new potential energy surfaces for the ground and the excited electronic state. The results are in excellent agreement with experimental data and the most recent reflection principle based model (Chen et al., 2010).

On the important low-energy side of the absorption band the isotopic fractionation increases with increasing wavelength and decreases with temperature. The former can be explained in terms of overall blue-shifting and an additional narrowing of the cross sections for the heavy isotopes, making photolysis slower for these isotopes on the low energy side. The decrease of fractionation with temperature is due to the vibrationally excited states; UV absorption from the excited vibrational states enhances the low energy side of the cross section, increasing the rate of photolysis in this region. At the same time the vibrationally excited states become more rapidly populated for the heavy isotopologues, thus decreasing the magnitude of the fractionation constant.

In the long wavelength region, i.e. $\lambda > 210$ nm, photolysis from highly excited vibrational states such as the 3rd bending excitation or the first combination state become important. These states are significant for describing the fractionation constants around room temperature.

It is shown that the experimentally observed wavelength dependence in the three-isotope exponent, β, is due to coincidental matching of the ArF laser frequency with structure in the cross sections caused by large amplitude bending and NN stretching motion.

In conclusion, this study indicates that photolysis contributes only very little to the mass independent oxygen isotope anomaly observed in tropospheric N_2O.

Supplementary material related to this article is available online at: http://www.atmos-chem-phys.net/11/8965/2011/acp-11-8965-2011-supplement.zip.

Acknowledgements. We thank Chris McLinden for providing us with the actinic flux data and Jan Kaiser for providing us with experimental data and the lamp spectral data. JAS also thanks W.-C. Chen and R. A. Marcus for useful discussions in the early and final stages of this study. We thank the IntraMIF project in the European Community's Seventh Framework Programme (FP7/2007-1013) under grant agreement number 237890 for support.

Edited by: J. Kaiser

References

Assonov, S. S. and Brenninkmeijer, C. A. M.: Reporting small $\Delta^{17}O$ values: existing definitions and concepts, Rapid Commun. Mass Spectrom., 19, 627–636, doi:10.1002/rcm.1833, 2005.

Chen, W.-C., Prakash, M. K., and Marcus, R. A.: Isotopomer fractionation in the UV photolysis of N_2O: 2. Further comparison of theory and experiment, J. Geophys. Res., 113, D05309, doi:10.1029/2007JD009180, 2008.

Chen, W.-C., Nanbu, S., and Marcus, R. A.: Isotopomer Fractionation in the UV Photolysis of N_2O: 3. 3D Ab Initio Surfaces and Anharmonic Effects, J. Phys. Chem. A, 114, 9700–9708, doi:10.1021/jp101691r, 2010.

Cliff, S. S. and Thiemens, M. H.: The $^{18}O/^{16}O$ and $^{17}O/^{16}O$ Ratios in Atmospheric Nitrous Oxide: A Mass-Independent Anomaly, Science, 278, 1774–1776, doi:10.1126/science.278.5344.1774, 1997.

Daud, M. N., Balint-Kurti, G. G., and Brown, A.: Ab initio potential energy surfaces, total absorption cross sections, and prod-

uct quantum state distributions for the low-lying electronic states of N_2O, J. Chem. Phys., 122, 054305, doi:10.1063/1.1830436, 2005.

Dunning Jr., T. H.: Gaussian basis sets for use in correlated molecular calculations. I. The atoms boron through neon and hydrogen, J. Chem. Phys., 90, 1007–1023, doi:10.1063/1.456153, 1989.

Forster, P., Ramaswamy, V., Artaxo, P., Berntsen, T., Betts, R., Fahey, D. W., Haywood, J., Lean, J., Lowe, D. C., Myhre, G., Nganga, J., Prinn, R., Raga, G., Schulz, M., and Van Dorland, R.: Climate Change 2007: The Physical Science Basis. Contribution of Working Group I to the Fourth Assessment Report of the Intergovernmental Panel on Climate Change, Cambridge University Press, 2007.

Hopper, D. G.: Ab initio multiple root optimization MCSCF study of the $C_{\infty v}/C_s$ excitation spectra and potential energy surfaces of N_2O, J. Chem. Phys., 80, 4290–4316, doi:10.1063/1.447260, 1984.

Johnson, M. S., Billing, G. D., Gruodis, A., and Janssen, M. H. M.: Photolysis of Nitrous Oxide Isotopomers Studied by Time-Dependent Hermite Propagation, J. Phys. Chem. A, 105, 8672–8680, doi:10.1021/jp011449x, 2001.

Johnston, J. C., Cliff, S. S., and Thiemens, M. H.: Measurement of multioxygen isotopic ($\delta^{18}O$ and $\delta^{17}O$) fractionation factors in the stratospheric sink reactions of nitrous oxide, J. Geophys. Res., 100, 16801–16804, doi:10.1029/95JD01646, 1995.

Kaiser, J. and Röckmann, T.: Absence of isotope exchange in the reaction of N_2O + $O(^1D)$ and the global $\Delta^{17}O$ budget of nitrous oxide, Geophys. Res. Lett., 32, L15808, doi:10.1029/2005GL023199, 2005.

Kaiser, J., Röckmann, T., and Brenninkmeijer, C. A. M.: Temperature dependence of isotope fractionation in N_2O photolysis, Phys. Chem. Chem. Phys., 4, 4420–4430, doi:10.1039/B204837J, 2002.

Kaiser, J., Röckmann, T., Brenninkmeijer, C. A. M., and Crutzen, P. J.: Wavelength dependence of isotope fractionation in N_2O photolysis, Atmos. Chem. Phys., 3, 303–313, doi:10.5194/acp-3-303-2003, 2003.

Kaiser, J., Röckmann, T., and Brenninkmeijer, C. A. M.: Contribution of mass dependent fractionation to the oxygen isotope anomaly of atmospheric nitrous oxide, J. Geophys. Res., 109, D03305, doi:10.1029/2003JD004088, 2004.

Kawamata, H., , Kohguchi, H., Nishide, T., and Suzuki, T.: Photodissociation of nitrous oxide starting from excited bending levels, J. Chem. Phys., 125, 133312, doi:10.1063/1.2264362, 2006.

Kim, K.-R. and Craig, H.: Nitrogen-15 and Oxygen-18 Characteristics of Nitrous Oxide: A Global Perspective, Science, 262, 1855–1857, doi:10.1126/science.262.5141.1855, 1993.

Knowles, P. J. and Werner, H.-J.: An efficient second-order MC SCF method for long configuration expansions, Chem. Phys. Lett., 115, 259–267, doi:10.1016/0009-2614(85)80025-7, 1985.

Knowles, P. J. and Werner, H.-J.: An efficient method for the evaluation of coupling coefficients in configuration interaction calculations, Chem. Phys. Lett., 145, 514–522, doi:10.1016/0009-2614(88)87412-8, 1988.

Kosloff, D. and Kosloff, R.: A Fourier method solution for the time dependent Schrödinger equation as a tool in molecular dynamics, J. Comp. Phys., 52, 35–53, doi:10.1016/0021-9991(83)90015-3, 1983.

Kosloff, R. and Tal-Ezer, H.: A direct relaxation method for calculating eigenfunctions and eigenvalues of the Schrödinger equation on a grid, Chem. Phys. Lett., 127, 223–230, doi:10.1016/0009-2614(86)80262-7, 1986.

Langhoff, S. R. and Davidson, E. R.: Configuration interaction calculations on the nitrogen molecule, J. Quantum Chem., 8, 61–72, doi:10.1002/qua.560080106, 1974.

Łapiński, A., Spanget-Larsen, J., Waluk, J., and Radziszewski, J. G.: Vibrations of nitrous oxide: Matrix isolation Fourier transform infrared spectroscopy of twelve N_2O isotopomers, J. Chem. Phys., 115, 1757–1764, doi:10.1063/1.1383031, 2001.

Le Quéré, F. and Leforestier, C.: Quantum exact three-dimensional study of the photodissociation of the ozone molecule, J. Chem. Phys., 92, 247–253, doi:10.1063/1.458471, 1990.

Liang, M.-C. and Yung, Y. L.: Sources of the oxygen isotopic anomaly in atmospheric N_2O, J. Geophys. Res., 112, D13307, doi:10.1029/2006JD007876, 2007.

Liang, M.-C., Blake, G. A., and Yung, Y. L.: A semianalytic model for photoinduced isotopic fractionation in simple molecules, J. Geophys. Res., 109, D10308, doi:10.1029/2004JD004539, 2004.

McLinden, C. A., McConnell, J. C., Griffioen, E., and McElroy, C. T.: A vector radiative-transfer model for the Odin/OSIRIS project, Can. J. Phys., 80, 375–393, doi:10.1139/p01-156, 2002.

McLinden, C. A., Prather, M. J., and Johnson, M. S.: Global modeling of the isotopic analogues of N_2O: Stratospheric distributions, budgets, and the ^{17}O-^{18}O mass-independent anomaly, J. Geophys. Res., 108, 4233, doi:10.1029/2002JD002560, 2003.

Moore, H.: Isotopic measurement of atmospheric nitrogen compounds, Tellus, 26, 169–174, doi:10.1111/j.2153-3490.1974.tb01963.x, 1974.

Nanbu, S. and Johnson, M. S.: Analysis of the Ultraviolet Absorption Cross Sections of Six Isotopically Substituted Nitrous Oxide Species Using 3D Wave Packet Propagation, J. Phys. Chem. A, 108, 8905–8913, doi:10.1021/jp048853r, 2004.

Prakash, M. K., Weibel, J. D., and Marcus, R. A.: Isotopomer fractionation in the UV photolysis of N_2O: Comparison of theory and experiment, J. Geophys. Res., 110, D21315, doi:10.1029/2005JD006127, 2005.

Prather, M., Ehhalt, D., Dentener, F., Derwent, R., Dlugokencky, E., Holland, E., Isaksen, I., Katima, J., Kirchhoff, V., Matson, P., Midgley, P., and Wang, M.: Climate Change 2001: The Scientific Basis, Contribution of Working Group I to the Third Assessment Report of the Intergovernmental Panel on Climate Change, Cambridge University Press, 2001.

Rahn, T. and Wahlen, M.: Stable Isotope Enrichment in Stratospheric Nitrous Oxide, Science, 278, 1776–1778, doi:10.1126/science.278.5344.1776, 1997.

Ravishankara, A. R., Daniel, J. S., and Portmann, R. W.: Nitrous Oxide (N_2O): The Dominant Ozone-Depleting Substance Emitted in the 21st Century, Science, 326, 123–125, doi:10.1126/science.1176985, 2009.

Röckmann, T., Brenninkmeijer, C. A. M., Wollenhaupt, M., Crowley, J. N., and Crutzen, P. J.: Measurement of the isotopic fractionation of $^{15}N^{14}N^{16}O$, $^{14}N^{15}N^{16}O$ and $^{14}N^{14}N^{18}O$ in the UV photolysis of nitrous oxide, Geophys. Res. Lett., 27, 1399–1402, doi:10.1029/1999GL011135, 2000.

Röckmann, T., Kaiser, J., Brenninkmeijer, C. A. M., Crowley, J. N., Borchers, R., Brand, W. A., and Crutzen, P. J.: Isotopic enrichment of nitrous oxide ($^{15}N^{14}N^{16}O$, $^{14}N^{15}N^{16}O$, $^{14}N^{14}N^{18}O$) in the stratosphere and in the laboratory, J. Geophys. Res., 106,

10403–10410, doi:10.1029/2000JD900822, 2001a.

Röckmann, T., Kaiser, J., Crowley, J. N., Brenninkmeijer, C. A. M., and Crutzen, P. J.: The origin of the anomalous or mass independent oxygen isotope fractionation in tropospheric N_2O, Geophys. Res. Lett., 28, 503–506, doi:10.1029/2000GL012295, 2001b.

Rontu Carlon, N., Papanastasiou, D. K., Fleming, E. L., Jackman, C. H., Newman, P. A., and Burkholder, J. B.: UV absorption cross sections of nitrous oxide (N_2O) and carbon tetrachloride (CCl_4) between 210 and 350 K and the atmospheric implications, Atmos. Chem. Phys., 10, 6137–6149, doi:10.5194/acp-10-6137-2010, 2010.

Schinke, R.: Photodissociation Dynamics, Cambridge University Press, 1993.

Schinke, R.: Photodissociation of N_2O: Potential energy surfaces and absorption spectrum, J. Chem. Phys., 134, 064313, doi:10.1063/1.3553377, 2011a.

Schinke, R.: Photodissociation of N_2O: Temperature dependence, Chem. Phys., In Press, Corrected Proof, doi:10.1016/j.chemphys.2011.06.003, 2011b.

Schinke, R., Suarez, J., and Farantos, S. C.: Communication: Photodissociation of N_2O – Frustrated NN bond breaking causes diffuse vibrational structures, J. Chem. Phys., 133, 091103, doi:10.1063/1.3479391, 2010.

Schmidt, B. and Lorenz, U.: WavePacket 4.6: A program package for quantum-mechanical wavepacket propagation and time-dependent spectroscopy, available via http://wavepacket.sourceforge.net, 2009.

Schmidt, J. A., Johnson, M. S., Lorenz, U., McBane, G. C., and Schinke, R.: Photodissociation of N_2O: Energy partitioning, J. Chem. Phys., 135, 024311, doi:10.1063/1.3602324, 2011.

Selwyn, G. S. and Johnston, H. S.: Ultraviolet absorption spectrum of nitrous oxide as a function of temperature and isotopic substitution, J. Chem. Phys., 74, 3791–3803, doi:10.1063/1.441608, 1981.

Simonaitis, R., Greenberg, R. I., and Heicklen, J.: The photolysis of N_2O at 2139 Å and 1849 Å, Int. J. Chem. Kinet., 4, 497–512, doi:10.1002/kin.550040504, 1972.

Tal-Ezer, H. and Kosloff, R.: An accurate and efficient scheme for propagating the time dependent Schrödinger equation, J. Chem. Phys., 81, 3967–3971, doi:10.1063/1.448136, 1984.

Toyoda, S., Yoshida, N., Urabe, T., Aoki, S., Nakazawa, T., Sugawara, S., and Honda, H.: Fractionation of N_2O isotopomers in the stratosphere, J. Geophys. Res., 106, 7515–7522, doi:10.1029/2000JD900680, 2001.

Turatti, F., Griffith, D. W. T., Wilson, S. R., Esler, M. B., Rahn, T., Zhang, H., and Blake, G. A.: Positionally dependent ^{15}N fractionation factors in the UV photolysis of N_2O determined by high resolution FTIR spectroscopy, Geophys. Res. Lett., 27, 2489–2492, doi:10.1029/2000GL011371, 2000.

von Hessberg, P., Kaiser, J., Enghoff, M. B., McLinden, C. A., Sorensen, S. L., Röckmann, T., and Johnson, M. S.: Ultra-violet absorption cross sections of isotopically substituted nitrous oxide species: $^{14}N^{14}NO$, $^{15}N^{14}NO$, $^{14}N^{15}NO$ and $^{15}N^{15}NO$, Atmos. Chem. Phys., 4, 1237–1253, doi:10.5194/acp-4-1237-2004, 2004.

Werner, H.-J. and Knowles, P. J.: A second order multiconfiguration SCF procedure with optimum convergence, J. Chem. Phys., 82, 5053–5063, doi:10.1063/1.448627, 1985.

Werner, H.-J. and Knowles, P. J.: An efficient internally contracted multiconfiguration-reference configuration interaction method, J. Chem. Phys., 89, 5803–5814, doi:10.1063/1.455556, 1988.

Yoshida, N. and Toyoda, S.: Constraining the atmospheric N_2O budget from intramolecular site preference in N_2O isotopomers, Nature, 405, 330–334, doi:10.1038/35012558, 2000.

Yung, Y. L. and Miller, C. E.: Isotopic Fractionation of Stratospheric Nitrous Oxide, Science, 278, 1778–1780, doi:10.1126/science.278.5344.1778, 1997.

Zhang, H., Wennberg, P. O., Wu, V. H., and Blake, G. A.: Fractionation of $^{14}N^{15}N^{16}O$ and $^{15}N^{14}N^{16}O$ during photolysis at 213 nm, Geophys. Res. Lett., 27, 2481–2484, doi:10.1029/1999GL011236, 2000.